NORTHWESTERN UNIVERSITY

Sandia National Laboratories

# Predictive Characterization of Aging and Degradation of Reactor Materials in Extreme Environments

**Jianmin Qu***
Northwestern University

**Remi Dingreville and Khalid Hattar**
Sandia National Laboratories**

Supported by NEET through DE-NE0000678

* Now with Tufts University

** Sandia National Laboratories is a multi-program laboratory managed and operated by Sandia Corporation, a wholly owned subsidiary of Lockheed Martin Corporation, for the U.S. Department of Energy's National Nuclear Security Administration under contract DE-AC04-94AL85000.

# Outline

- Project Objectives and Scopes
- Accomplishments to Date
  - Deliverables and Publications
- Examples of Recent Results
  - Cavity Evolution at Grain Boundaries as a Function of Radiation Damage and Thermal Conditions in Nanocrystalline Nickel
  - Depth-Dependent Hardness of Ion Irradiated Materials

**Objective:**

Develop a suite of unique experimental techniques, augmented by a mesoscale computational framework, to understand and predict the long-term effects of irradiation, temperature, and stress on materials microstructures and their macroscopic behavior.

**Scope:**

The experimental techniques and computational tools will be demonstrated on two distinctive types of reactor materials, namely, Zr alloys (Zircaloy-4) and high-Cr martensitic steels (HT9). These materials are chosen as the testbeds because they are the archetypes of high-performance reactor materials (cladding, wrappers, ducts, pressure vessel, piping, etc.).

# **Deliverables** (Since Last Review)

Completion data: 12/19/2015
Deliverable: Provide status of In situ TEM under Heavy Ion Irradiation and Helium Implantation

Completion data: 12/19/2015
Deliverable: Issue status of status on developing chemo-mechanics framework for microstructure evolution

Completion data: 12/19/2015
Deliverable: Formulating a Mesoscale Model for Simulating Microstructure Evolution during Aging

Completion data: 12/19/2015
Deliverable: Second Annual Progress Report on Predictive Characterization of Aging & Degradation of Reactor Materials in Extreme Environments

Completion date: 3/30/2016
Deliverable: Quantitative evaluation of aging vs. microstructure during ion irradiation

Completion data: 6/19/2016
Deliverable: Understanding the synergistic effects on defect interactions

# Publications

1. B. Muntifering, S. J. Blair, C. G., A. Dunn, R. Dingreville, J. Qu, K. Hattar., 2015, Cavity Evolution at Grain Boundaries as a Function of Radiation Damage and Thermal Conditions in Nanocrystalline Nickel. *Materials Research Letters*. Vol. 4, pp. 96-103.
2. B. Muntifering, R. Dingreville, K. Hattar and J. Qu, 2015. Electron Beam Effects during In-Situ Annealing of Self-Ion Irradiated Nanocrystalline Nickel. *MRS Proceedings*, 1809, mrss15-2136630 doi:10.1557/opl.2015.499.
3. Muntifering, B., Dunn, A., Dingreville, R., Qu, J., and Hattar, K., 2016, "In-Situ TEM He+ Implantation and Thermal Aging of Nanocrystalline Fe," *Microscopy and Microanalysis*, Vol. 21(Suppl. 3), pp 113-114.
4. A. Dunn, R. Dingreville, L. Capolungo, 2015, "Multi-scale simulation of radiation damage accumulation and subsequent hardening in neutron-irradiated α-Fe. *Modelling and Simulation in Materials Science and Engineering*, Vol. 24, pp. 015005.

# Cavity Evolution at Grain Boundaries as a Function of Radiation Damage and Thermal Conditions in Nanocrystalline Nickel

(Materials Research Letters, Vol. 4, pp. 96-103, 2015)

**Hypothesis:** The high GB/volume ratio in nanostructured materials enhances radiation tolerance because the GBs absorb irradiation-induced defects.

**Model Material:** Nanocrystalline Ni film (PLD)

**Tools:** in situ ion irradiation TEM ($I^3$TEM) facility at SNL, and coupled chemo-mechanics modeling.

**Samples:** Electron transparent nanocrystalline nickel films were produced by PLD to a thickness of approximately 80 nm on a NaCl substrate at nominally room temperature. The salt substrate was then dissolved in a deionized water bath to obtain freestanding nickel films, which were then floated onto a copper clamshell transmission electron microscope (TEM) grid. To establish columnar grain structure, the films were annealed at 550°C for 5 min, resulting in a strong {100} texture.

**Irradiation:** two sequences

1. $Ni^{3+}$ followed by $He^{+}$
2. $He^{+}$ followed by $Ni^{3+}$

Table 1. Self-ion irradiation and helium implantation parameters.

| | $Ni^{3+}$ Rate | $Ni^{3+}$ Dose | Damage | $He^{+}$ Rate | $He^{+}$ Dose | Damage | Total damage |
|---|---|---|---|---|---|---|---|
| Sequence | $Ni^{3+}/cm^2s$ | $Ni^{3+}/cm^2$ | DPA | $He^{+}/cm^2s$ | $He^{+}/cm^2$ | DPA | DPA |
| $Ni^{3+}$, $He^{+}$ | $1.5 \times 10^{11}$ | $5.4 \times 10^{14}$ | $\approx 1.8$ | $10^{13}$ | $2 \times 10^{16}$ | $\approx 1.5$ | $\approx 3.3$ |
| $He^{+}$, $Ni^{3+}$ | $1.5 \times 10^{11}$ | $2.7 \times 10^{14}$ | $\approx 0.9$ | $10^{13}$ | $8 \times 10^{16}$ | $\approx 5.5$ | $\approx 6.4$ |

(1) $Ni^{3+}$ followed by $He^{+}$

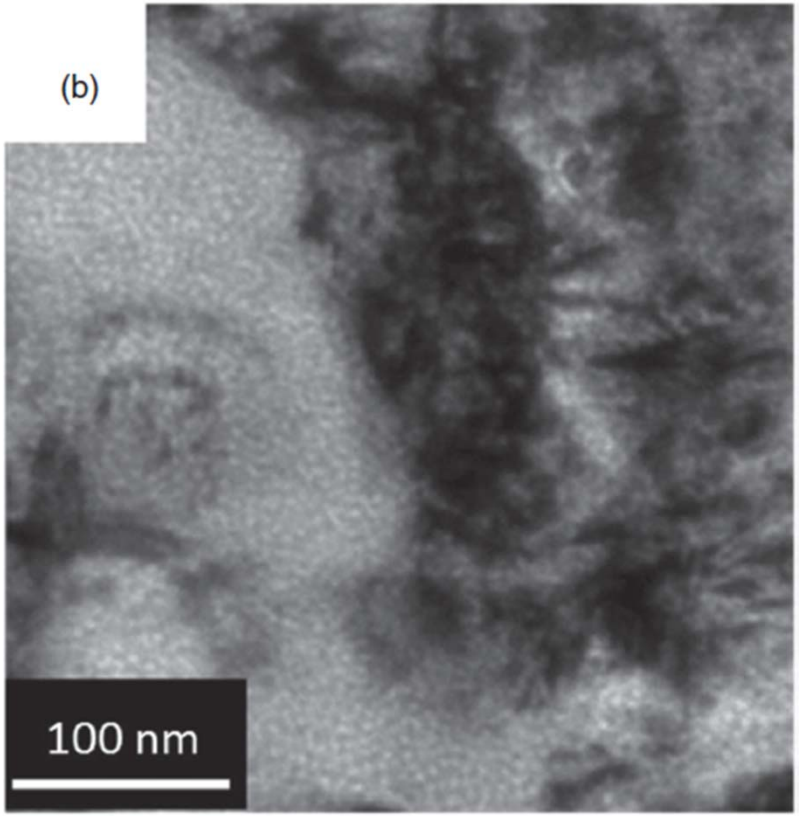


(2) $He^{+}$ followed by $Ni^{3+}$

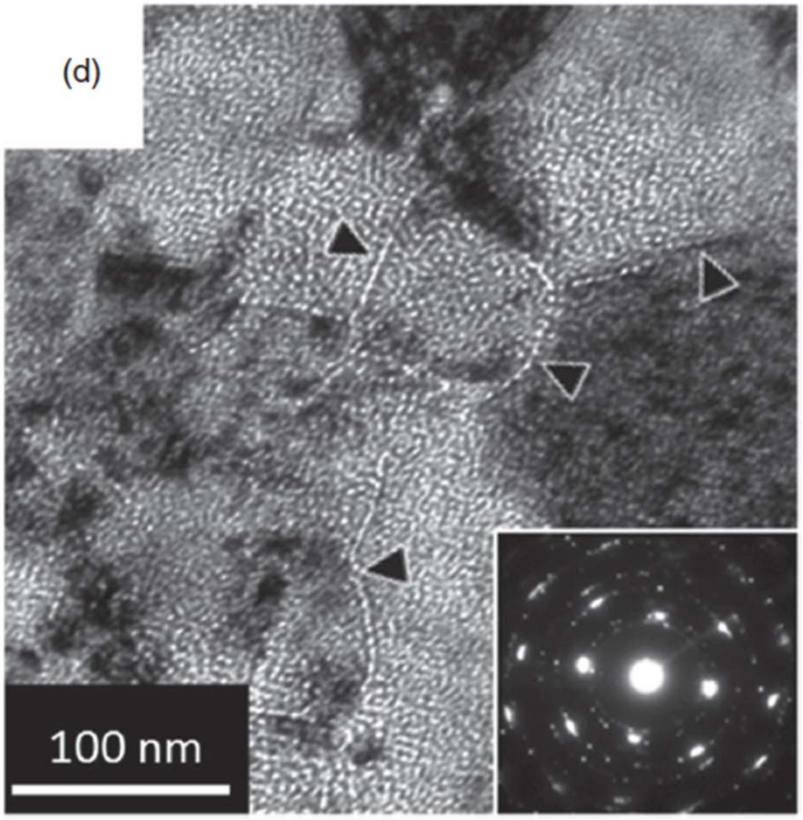


**Observations:**

Although both cases have uniform voids everywhere, case (2) has much higher void concentration on the GBs.

# Post-Irradiation Annealing

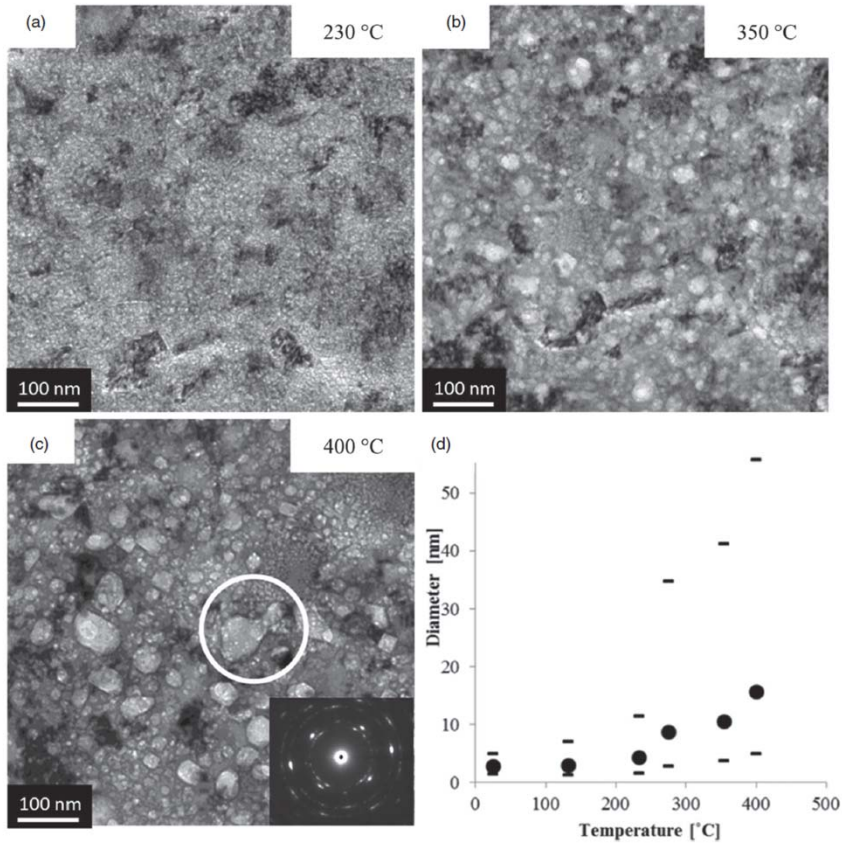


These experiments were done in-situ, with a ramp rate of about 5C/min. They were not necessarily held at temperature for any specific amount of time, just long enough to capture an image, so maybe 2 minutes at each imaged temperature.

**Observations:**

- $H^+$ bubbles attracted mobile vacancies and transformed into cavities.
- Cavities grow via coalescence.
- Some cavities grew as large as or larger than the grains themselves.
- No preferential cavity growth between grain and GBs.
- GBs did not significantly stabilize the cavities on them.

# Conclusions

- The order of the irradiation and implantation has a significant impact on the distribution of the resulting cavity structure.
- $He^{+}$ followed by $Ni^{3+}$ results in much higher vacancy concentration on the GBs.
- The difference is due to the fact that self-irradiation provides additional sink locations for the helium to cluster uniformly without having to migrate to the grain boundaries or surfaces.
- Post-irradiation annealing shows that vacancies on the GB are no more thermally stable than those inside the grain.
- Single component nanocrystalline metals dominated by low-angle grain boundaries will not provide significant radiation tolerance compared to large grained systems.

# Chemo-Mechanics Model

Chemical potential:

$$\mu_\alpha = \mu_\alpha^{(0)} + RTln(\gamma_\alpha c_\alpha) - V_m \eta_\alpha \sigma_{kk}$$

Flux: $J_\alpha = -\frac{D_\alpha c_\alpha}{RT} \nabla \cdot \mu_\alpha$

Chemical equilibrium:

$$\frac{\partial c_\alpha}{\partial t} = -\nabla \cdot J_\alpha + \sum_\beta a_{\alpha\beta} f_\beta$$

Mechanical equation:

$$\sigma_{ji,j}^{(e)} = 0$$

Strain decomposition:

$$\hat{\varepsilon}_{ij} = \varepsilon_{ij}^{(e)} + \varepsilon_{ij}^{(c)}$$

Compositional eigenstrain:

$$\varepsilon_{ij}^{(c)} = \delta_{ij}(\eta_I c_I + \eta_V c_V)$$

Defect-defect interaction rates:

$$f_{defect-defect} = Z_{int}\omega\left(n_i^{\frac{1}{3}} + n_j^{\frac{1}{3}}\right)(D_i + D_j)c_i c_j$$

Individual defect dissociation rate: $f_{dissociation} = \omega n^{\frac{1}{3}} D_\alpha e^{-\frac{E_b^{(\alpha)}(n)}{k_b T}} N$

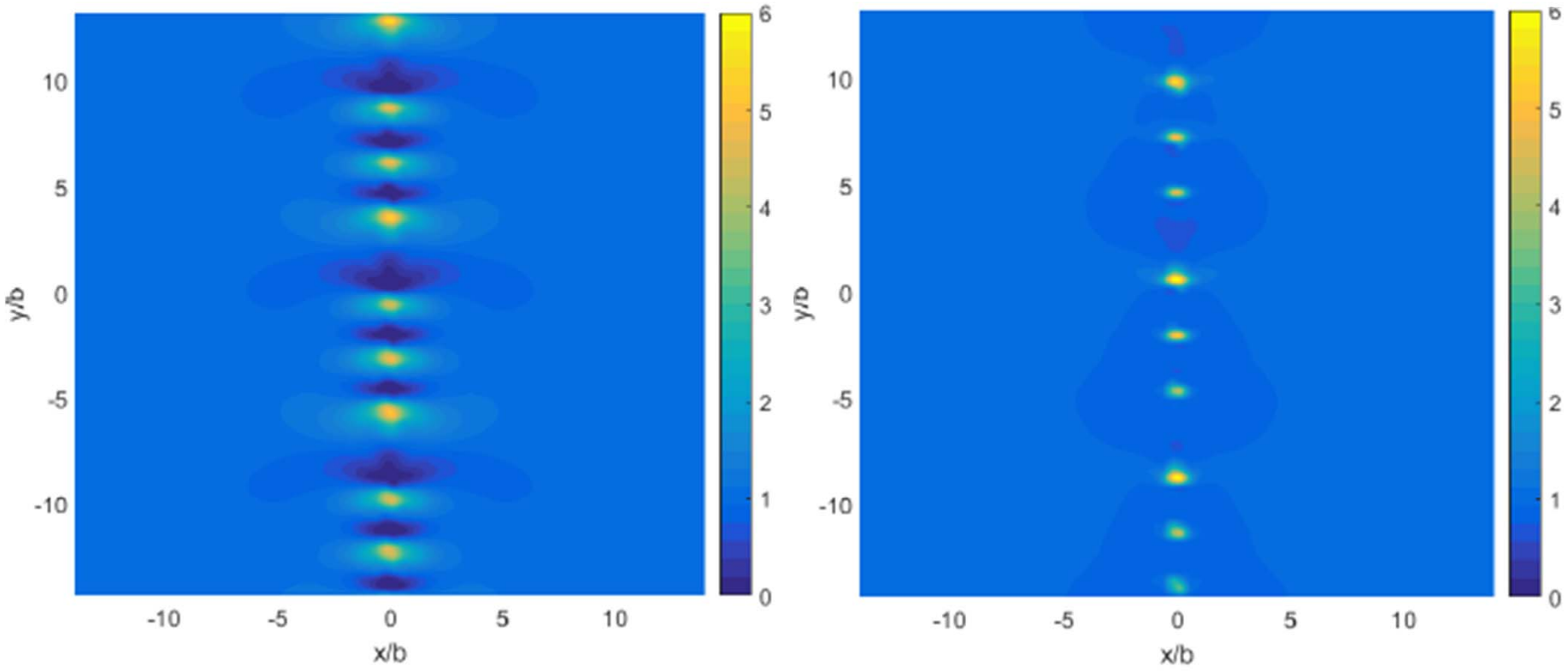


(a) SIAs (b) Vacancies

Normalized concentrations $c_\alpha/c_0$ for a $\Sigma 85$, 25.06° grain boundary constructed using disclination dipoles. Spatial axes are normalized by the Burgers vector $b$.

# Conclusions

- A chemo-mechanics model was developed to study radiation-induced segregation (RIS). In this way, RIS has been modeled as a two-way interaction between intrinsic stress and point defects, causing hydrostatic stress to be relieved while point defects are accumulated and/or depleted.
- The resulting segregation profiles are non-uniform along the GBs with alternating regions of enrichment and depletion.
- Averaging the segregation along the length of the grain boundaries reveals W-shaped vacancy segregation profiles, predicting void-denuded zones near grain boundaries due to annihilation with large concentrations of SIAs.

# Depth-Dependent Hardness of Ion Irradiated Metals

(*J. Nuclear Material*, to be submitted)

**Purposes:** Investigate the depth-dependent hardness of ion irradiated materials, and develop a predictive model to simulate the depth-dependent hardness under different irradiation conditions.

**Model Materials:** Zircaloy-4 (Zr-4) and Optimized ZIRLO

**Tools:** Nanoindentation (iMicro Nanoindenter from Nanomechanics, Inc. , FEM (Abaqus) and micromechanics modeling.

# Samples and Irradiation Conditions

- Commercially available Zr-4 and Zirlo sheets were cut into 9mm×9mm×0.4mm pieces.
- One surface of the sample was polished on a lapping stage, first with SiC abrasive papers (from FEPA P600 to P4000 grades), then with different silica suspensions from 1 µm to 0.05 µm.
- Sample were then irradiated at room temp with 24 MeV $Zr^{4+}$ ions at an average rate of 4.8E10 ions/($cm^2$s) for 5 hrs and 61 hrs, respectively.
- During the irradiation, half of the polished surface of each sample was masked by an aluminum foils so only the unmasked half was irradiated.

# Hardness of Zr-4 Samples after 61 hours of Irradiation

Sample (a)

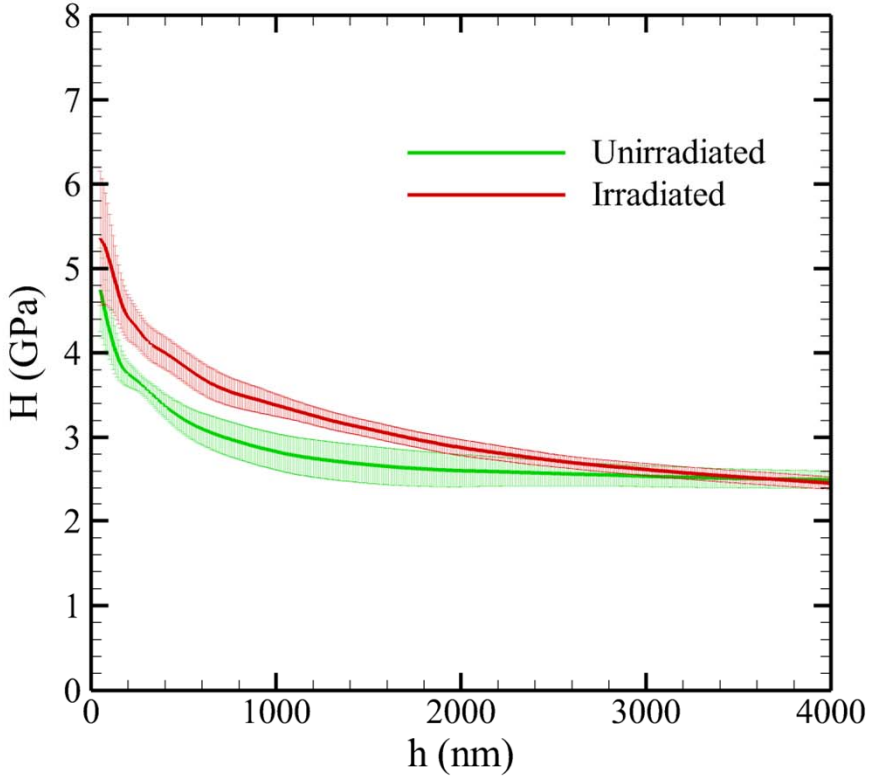


Sample (b)

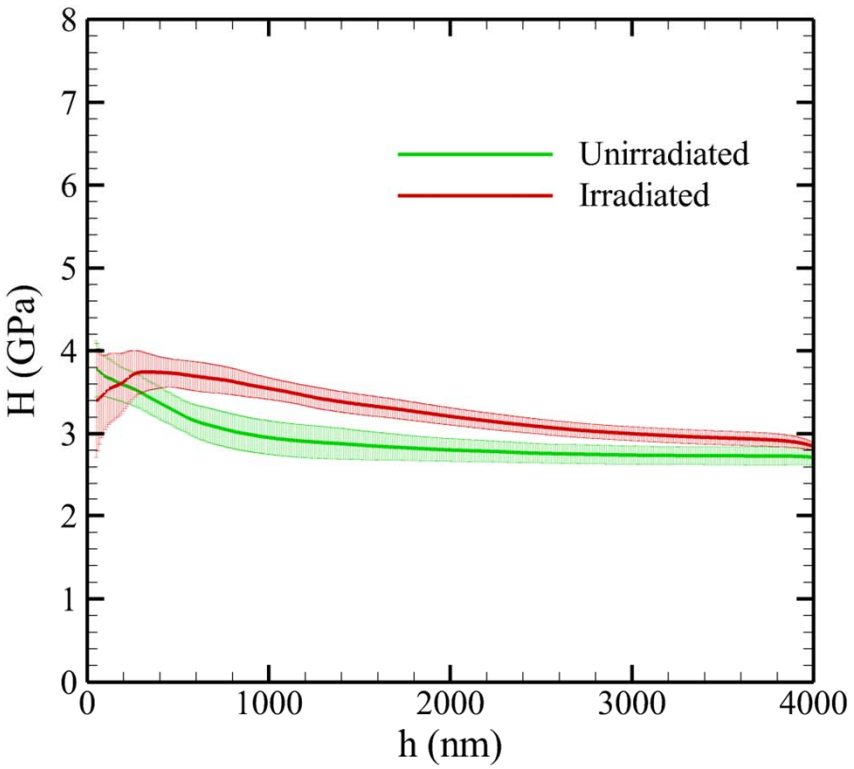

# Modeling Depth-Dependent Hardness

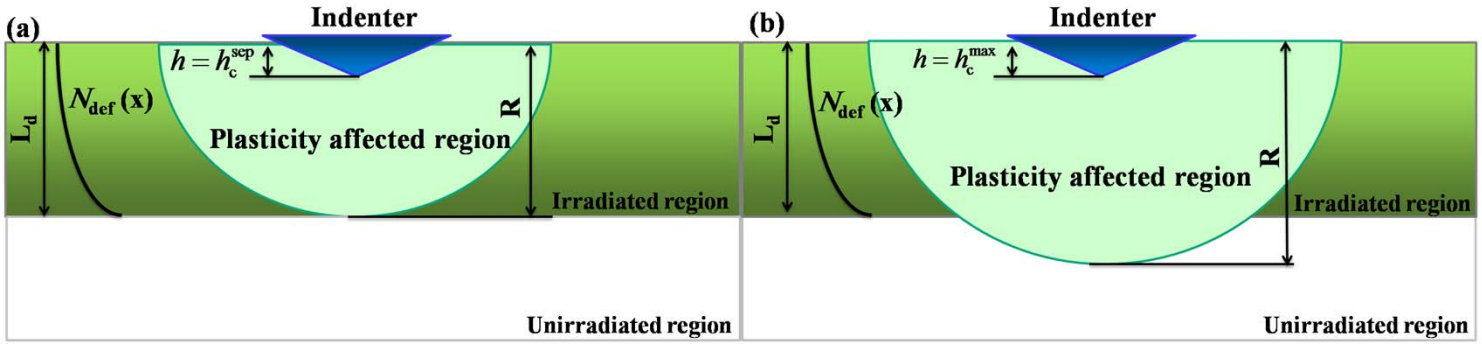


$$H_{irr} = H_0\sqrt{1+\frac{h^*}{Mh}+\frac{A^2h^*(Mh)^n}{(n+1)(n+3)L_d^{\,n+1}}} \quad \text{for} \quad h \le h_c^{sep}$$

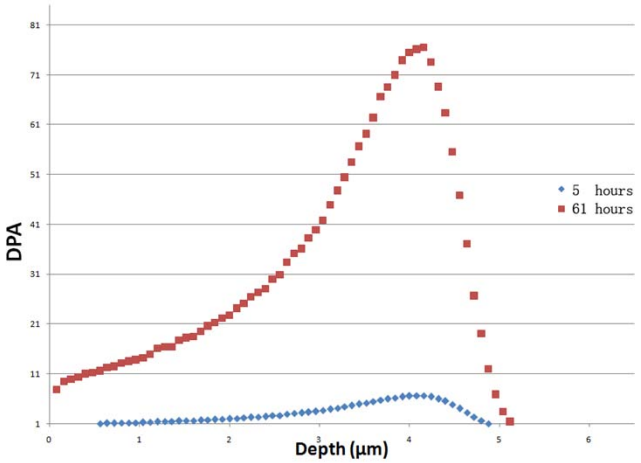


$$H_{irr} = H_0\sqrt{1+\frac{h^*}{Mh}+\frac{A^2h^*}{2Mh}\left[\frac{1}{n+1}-\frac{L_d^2}{(n+3)(Mh)^2}\right]} \quad \text{for} \quad h > h_c^{sep}$$

$$\rho_{def}(x) = \begin{cases} \left(\frac{x}{L_d}\right)^n \rho_{def}^0, & x \le L_d \\ 0, & x > L_d \end{cases}$$

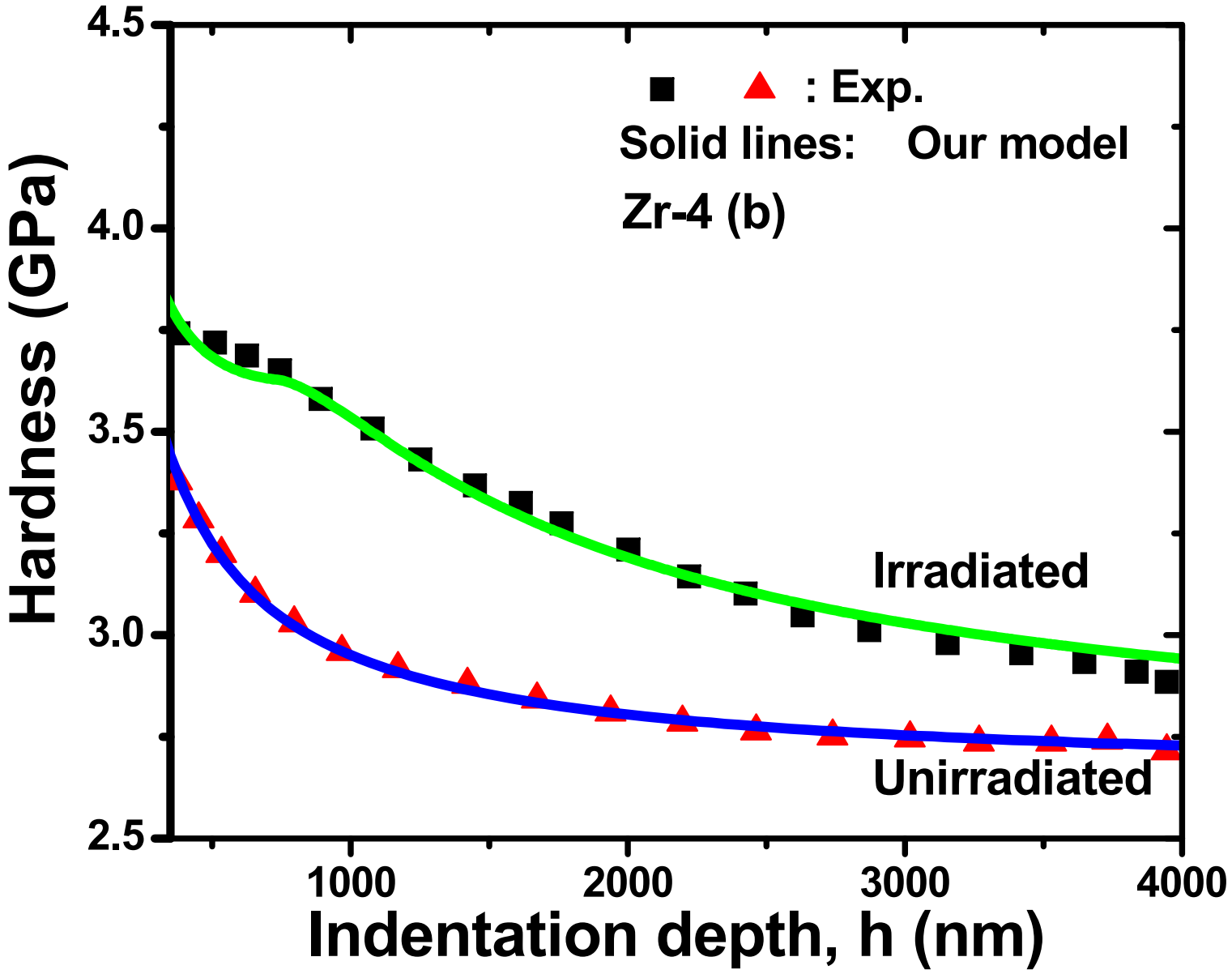
■ ▲ : Exp.
Solid lines: Our model
Zr-4 (b)
Irradiated
Unirradiated
Hardness (GPa)
4.5
4.0
3.5
3.0
2.5
1000
2000
3000
4000
Indentation depth, h (nm)

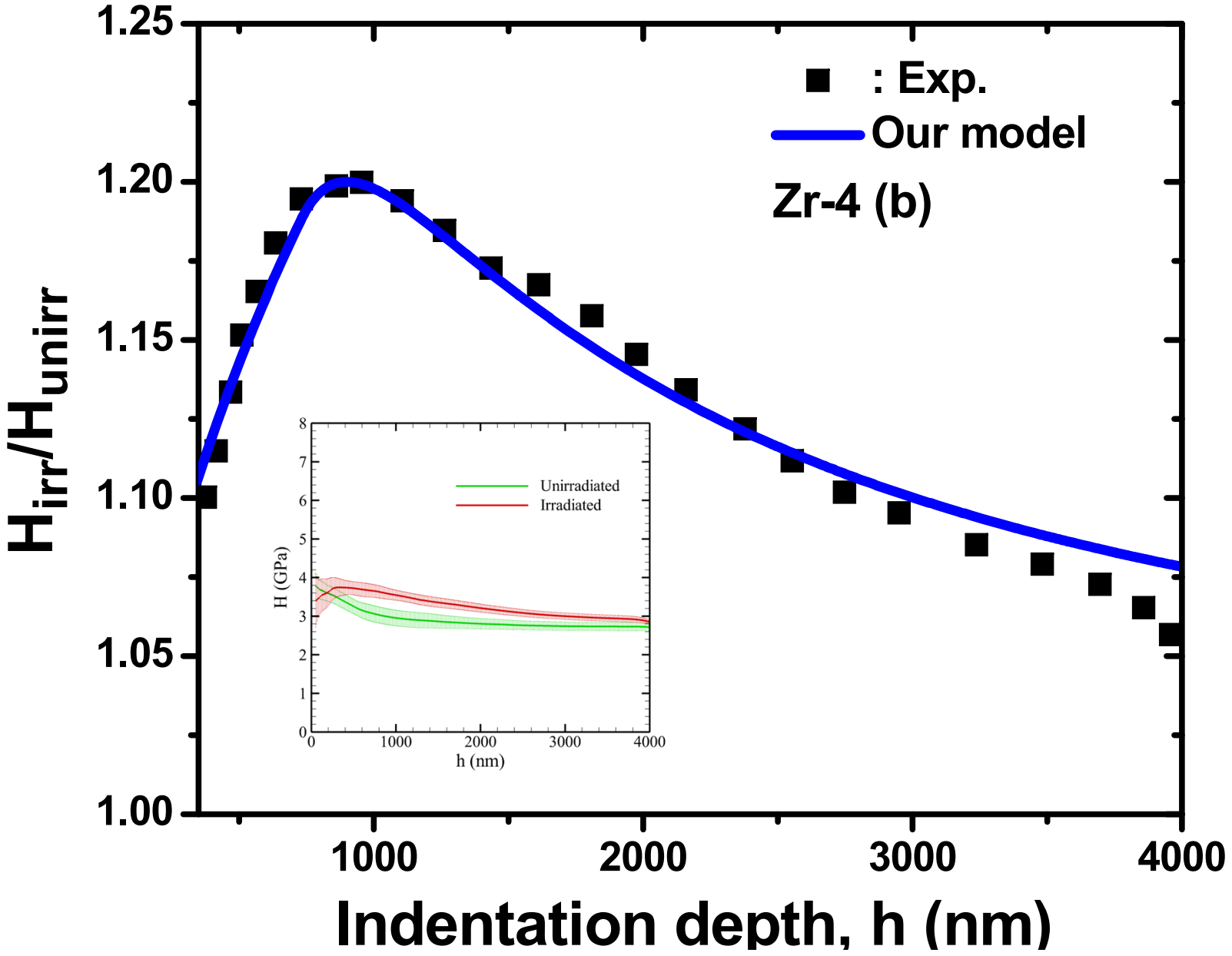
1.25
1.20
1.15
1.10
1.05
1.00
1000
2000
3000
4000
$H_{irr}/H_{unirr}$
Indentation depth, h (nm)
: Exp.
Our model
Zr-4 (b)
Unirradiated
Irradiated
H (GPa)
h (nm)
0
1000
2000
3000
4000
1
2
3
4
5
6
7
8

# Comparison with Literature Data on Stainless Steels

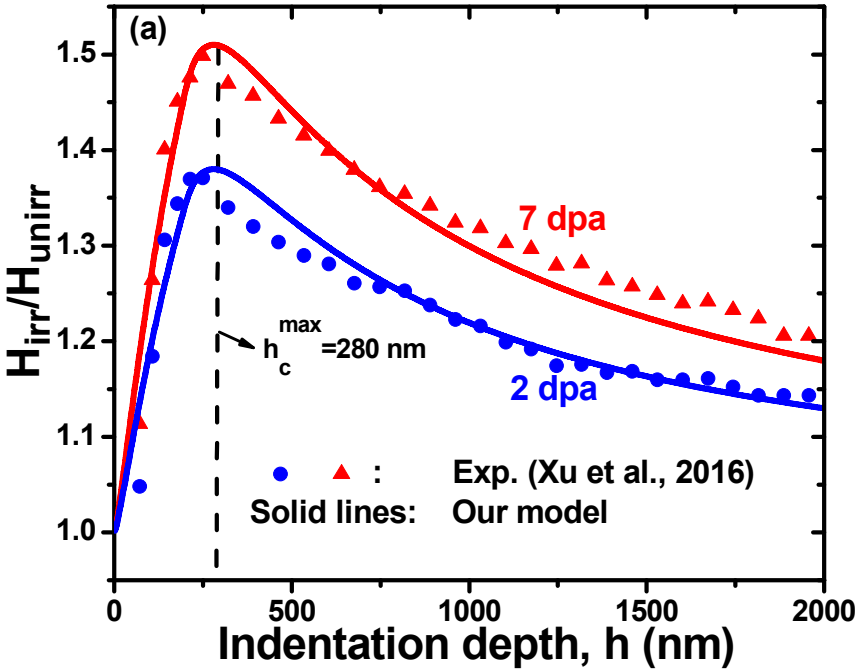


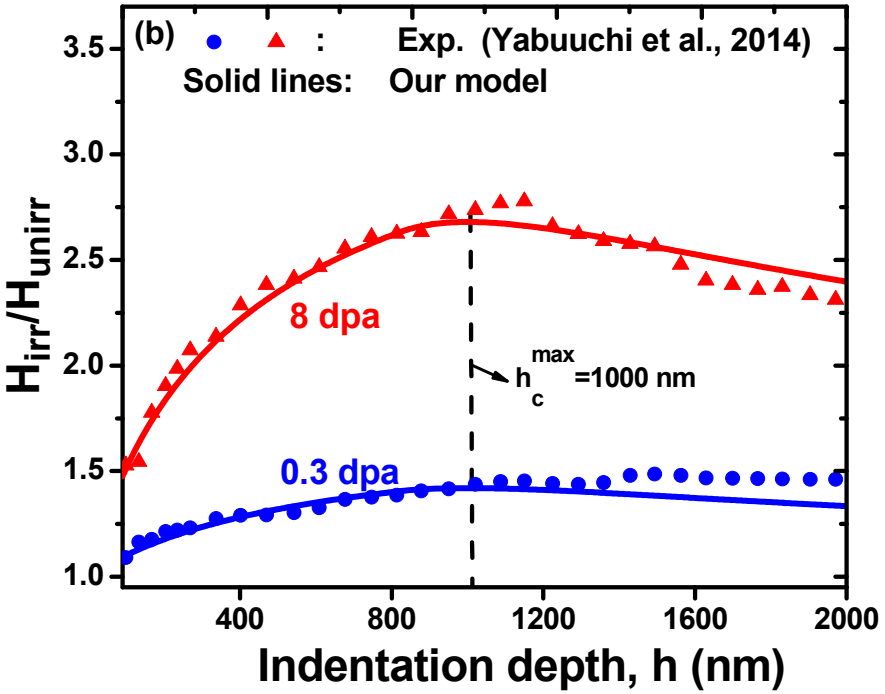

# Predictive Capability of the Model

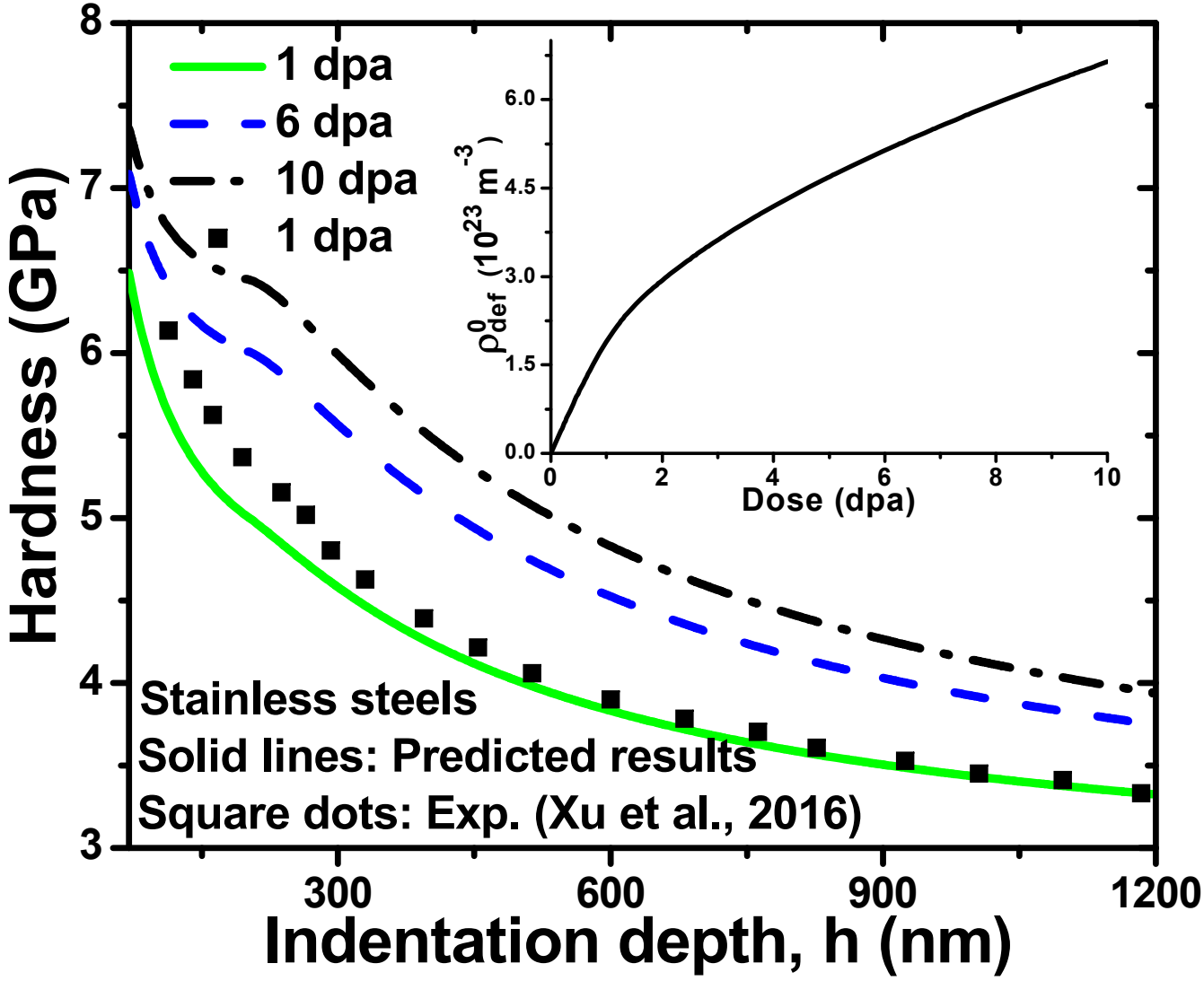

# Applications of the Model

$$H = f(h, n, \rho_{def}, L_d)$$

1. Predict the change in material hardness (which is related to yield strength) due to ion irradiation.
2. Characterize ion-irradiation induced defect density and distribution.

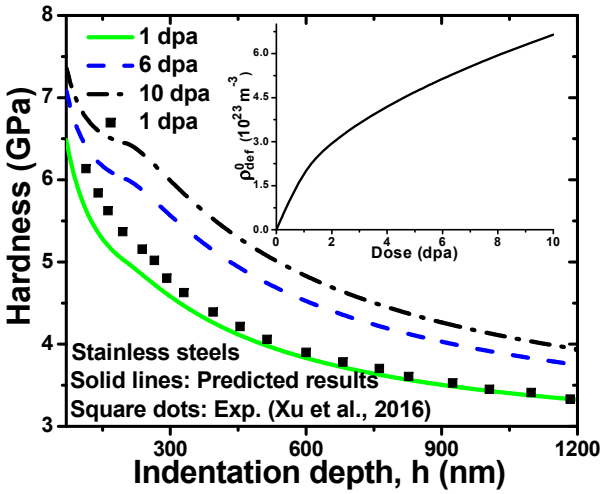


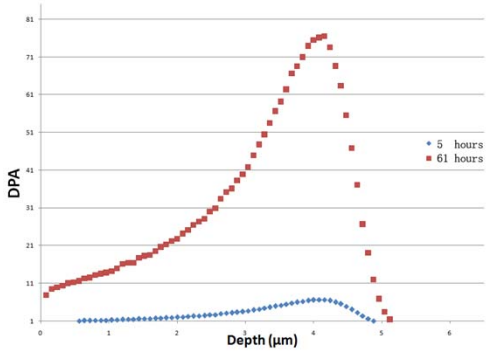


$$\rho_{\mathrm{def}}(x) = \begin{cases} \left(\frac{x}{L_{\mathrm{d}}}\right)^n \rho_{\mathrm{def}}^0, & x \le L_{\mathrm{d}} \\ 0, & x > L_{\mathrm{d}} \end{cases}$$